


Article

Energy and Environmental Assessment of a Hybrid Dish-Stirling Concentrating Solar Power Plant

Stefania Guarino ^{1,*} , Alessandro Buscemi ¹, Antonio Messineo ²  and Valerio Lo Brano ¹ 

¹ Department of Engineering, University of Palermo, 90128 Palermo, Italy; alessandro.buscemi@unipa.it (A.B.); valerio.lobrano@unipa.it (V.L.B.)

² Faculty of Engineering and Architecture, University of Enna “Kore”, Cittadella Universitaria, 94100 Enna, Italy; antonio.messineo@unikore.it

* Correspondence: stefania.guarino@unipa.it

Abstract: Although the 2019 global pandemic slowed the growing trend of CO₂ concentrations in the atmosphere, it has since resumed its rise, prompting world leaders to accelerate the generation of electricity from renewable sources. The study presented in this paper is focused on the evaluation of the energy and environmental benefits corresponding to the hypothesis of hybridizing a dish-Stirling plant installed on the university campus of Palermo (Italy). These analyses were carried out by means of dynamic simulations based on an accurate energy model validated with the experimental data collected during the measurement campaign that occurred during the period of operation of the reference plant. Assuming different scenarios for managing the production period and different fuels, including renewable fuels, it was found that the annual electricity production of the dish-Stirling system operating in solar mode can be increased by between 47% and 78% when hybridized. This would correspond to an increase in generation efficiency ranging from 4% to 16%. Finally, assuming that the dish-Stirling system is hybridized with renewable combustible gases, this would result in avoided CO₂ emissions of between approximately 1594 and 3953 tons over the 25-year lifetime of the examined plant.

Keywords: solar energy; concentrating solar power; dish-Stirling; hybridization; energy analysis; renewable fuel



Citation: Guarino, S.; Buscemi, A.; Messineo, A.; Lo Brano, V. Energy and Environmental Assessment of a Hybrid Dish-Stirling Concentrating Solar Power Plant. *Sustainability* **2022**, *14*, 6098. <https://doi.org/10.3390/su14106098>

Academic Editors: Luca Marchitto and Cinzia Tornatore

Received: 6 April 2022

Accepted: 16 May 2022

Published: 17 May 2022

Publisher's Note: MDPI stays neutral with regard to jurisdictional claims in published maps and institutional affiliations.



Copyright: © 2022 by the authors. Licensee MDPI, Basel, Switzerland. This article is an open access article distributed under the terms and conditions of the Creative Commons Attribution (CC BY) license (<https://creativecommons.org/licenses/by/4.0/>).

1. Introduction

The share of renewables in global electricity generation reached almost 29% in 2020 [1], and the renewable installed capacity amounted to 2.79 TW in the same year [2]. The predominant renewable resources in electricity generation are hydropower, wind, and solar power, which correspond to a share of renewable installed capacity of about 43%, 26%, and 25%, respectively [2]. Among solar energy technologies, concentrating solar power (CSP) systems efficiently generate electricity from solar energy using a thermodynamic cycle, such as Rankine, Brayton, or Stirling [3]. These technologies are very promising and are increasingly deployed worldwide, especially in countries located in the Sunbelt region (including countries in the Mediterranean, North and South Africa, China, India, Latin America, and Australia), as they are characterized by very high levels of direct normal irradiance (DNI) [4,5]. CSP systems mainly consist of a collector, which can be of different shapes and is designed to capture and subsequently concentrate the sun's rays onto a receiving system, a solar tracking system and a power conversion unit (PCU). These technologies can be classified into four further types, namely: parabolic troughs and Fresnel linear reflectors, which are defined as line-focusing technologies as their collectors linearly concentrate the solar radiation onto a receiver tube; and central towers and parabolic dish systems which are point-focusing technologies that have a collector that concentrates the solar radiation on a single point receiver [6].

Among these technologies, parabolic trough systems, solar towers and Fresnel linear reflectors are the most commercially mature, as they are characterized by high conversion efficiencies, can be coupled with thermal storage systems to generate electricity even during the hours when direct solar irradiation is not available, and do not emit greenhouse gases during their operation.

Dish-Stirling concentrators mainly comprise the paraboloidal shaped reflector that concentrates the sun's rays on a focal point where the receiver and the entire PCU are fixed, the biaxial tracking system, and the cooling system of the engine. The high-temperature thermal energy obtained is transferred to the Stirling engine for the production of mechanical energy, and this is finally converted into electricity by means of an electric generator [7]. When compared to other CSP technologies, dish-Stirling systems have the lowest commercial penetration although they feature the highest solar-to-electric conversion efficiency and geometric concentration ratios [8–13]. Indeed, some factors limit the competitiveness of dish-Stirling systems, and essentially these consist of the high installation cost [10,12] and the difficulty of coupling such systems to thermal storage systems [11].

In order to improve the market penetration of dish-Stirling systems, several theoretical and experimental studies have been conducted on both system optimization and the investigation of applications in various fields such as cogeneration, drinking water production, off-grid electrification, water pumping, thermal and electrical energy storage, and hybridization [13,14]. The hybridization of renewable electricity generation technologies, such as dish-Stirling systems, by exploiting different primary energy sources in addition to solar energy, would make it possible to extend the operating period and solve the problem of the aleatory and intermittent nature of the solar source. In this way, the hybridization of the CSP dish-Stirling systems would ensure more stable production, and therefore greater flexibility in meeting electricity demands, which do not always match the period of availability of solar radiation [15]. Furthermore, if the solar source is combined with another renewable energy source, it would be possible to achieve not only an increase in electricity production, but also a significant environmental benefit in terms of avoided CO₂ equivalent emissions.

Both theoretical and experimental studies have been carried out on the hybridization of dish-Stirling systems. Monné et al. carried out an energy analysis and life cycle assessment on two possible configurations of a 10 kW_e hybrid dish-Stirling system using natural gas and biogas considering Seville (Spain) as the climatic location. The data analysed showed that hybridization can be advantageous depending on the nature of the fuel used, and biogas is the best performing [16,17]. Hartenstine et al. studied the operation of a hybrid receiver by means of numerical simulations and demonstrated its technological feasibility through small-scale tests. The hybrid receiver was designed to achieve an overall thermal efficiency of at least 80%. The main objective of this development was to design, fabricate and demonstrate that a heat pipe receiver can operate using different energy sources, even simultaneously. A full-scale hybrid receiver was then fabricated, demonstrating the possibility of ensuring maximum and continuous electrical output from the system [18]. Within the same project, BIoSTIRLING-4SKA, Blázquez et al. performed the optimization of the concentrator geometry and receiver cavity according to the requirements of the flow distribution on the receiver walls set by the hybrid receiver designer [19], and Barbosa et al. tested hybridization with syngas produced from biomass [20]. Kang et al. experimentally investigated the heat transfer characteristics of the hybrid solar receiver for a concentrated dish system in order to achieve an improvement in energy and economic efficiency [21]. Laing et al. developed a hybrid sodium heat pipe receiver as part of the HYHPIRE project. The hybrid receiver was designed for the SBP/LCS 10-kW_e dish/Stirling system with the SOLO-161 Stirling engine. The system was successfully tested in all operating modes reaching generation efficiencies of 16% in solar-only mode, 17% in gas-only mode, and 15% in hybrid-mode with a maximum gross output power of 7.8 kW. A market-ready combustion system was developed for the SOLO 161 CHP engine, also demonstrating a reduced environmental impact [22]. Moreno et al. designed and tested a prototype of

a hybrid dish-Stirling combustion system. The system consisted of a pre-mixed natural gas burner that heats a finned sodium heat pipe. The experimentally validated design emphasised simplicity, low cost and robustness [23].

In this paper, a theoretical and parametric study is presented, aimed at evaluating and verifying the energy and environmental benefits that could be obtained by modifying the operating set-up of the dish-Stirling system installed at the university campus of Palermo, in Southern Italy, from solar to hybrid. The hybridization of this system, which already mounts a suitable engine for that purpose, will be the subject of future projects and experiments. The dish-Stirling system of Palermo, which was manufactured by the Swedish company Ripasso Energy, has a peak electrical power of 31.5 kW_e with a DNI of 960 W/m², and holds the current worldwide record for solar-to-electric conversion efficiency of 32% (a record set at the test site in Upington, South Africa) [11]. In this work, energy and environmental analyses were carried out by varying certain factors, such as: the operating strategy of the hybrid power plant, i.e., the number of hours per day during which the system operates in solar or hybrid mode; the installation site (with different levels of DNI); and the type of fuel gas used to supply the combustion unit. Specifically, the operation of the dish-Stirling system in hybrid configuration was investigated assuming the use of natural gas or biogas and syngas, both derived from lignocellulosic biomass. In addition to Palermo, the other two installation sites considered in this study already host two large CSP plants: the first, to the west of Abu Dhabi (United Arab Emirates), hosts Shams, which is the largest renewable energy project in operation in the Middle East, with a capacity of 100 MW [24]; and the second, in the Mojave Desert (California, United States), where the Mojave Solar Project (MSP), with a total power capacity of 250 MW, is installed [25]. To carry out the environmental analysis in the aforementioned locations, the energy and technological context of each country was taken into account to find a solution that can potentially push the system towards widespread use.

The paper is structured as follows:

- The second section defines and describes the energy model of the hybrid dish-Stirling system and the methodology used to carry out the environmental analysis of the same system.
- In the third section, the reference dish-Stirling system is described, and an overview of the different case studies investigated is illustrated, varying the installation location and the specific fuel gas used.
- The fourth section shows the results obtained in terms of both energy performance and achievable environmental benefits.
- Finally, in the fifth section, the conclusions of this research are drawn.

2. Materials and Methods

As mentioned above, dish-Stirling systems efficiently convert direct solar radiation into electrical energy. However, the intermittent and aleatory nature of the solar energy source makes the energy generation discontinuous and, therefore, it may not meet the energy demand of the end-user. Among the various CSP technologies, one of the advantages of solar concentrators driven by Stirling engines is that it can be powered by high-temperature thermal energy obtained from any type of energy source, whether renewable or not. The hybridization of Stirling engines would allow the solar plant to operate even in the absence of direct solar radiation; for example, at night or on days when the sky is not clear. Thus, the Stirling engine could be powered by thermal energy obtained from the concentration of direct solar radiation, or alternatively by thermal energy obtained from the combustion of fuel gases in an external combustion unit.

For this purpose, as shown in Figure 1 below, the hybrid dish-Stirling solar concentrator system layout should include the following additional components:

- The combustion unit including the combustion chamber, the ignition device, the fuel controller, and the burner.

- The fuel feeding system, i.e., the set of pipes and components required to transport the fuel used into the combustion unit.
- The fan supplying the air that is used as a comburent to the combustion chamber.
- The heat recovery unit, i.e., a heat exchanger capable of pre-heating the air delivered to the combustion chamber by recovering part of the residual heat from the exhaust gases.
- A control system that allows the switching of the operation mode of the dish-Stirling system from solar to hybrid.

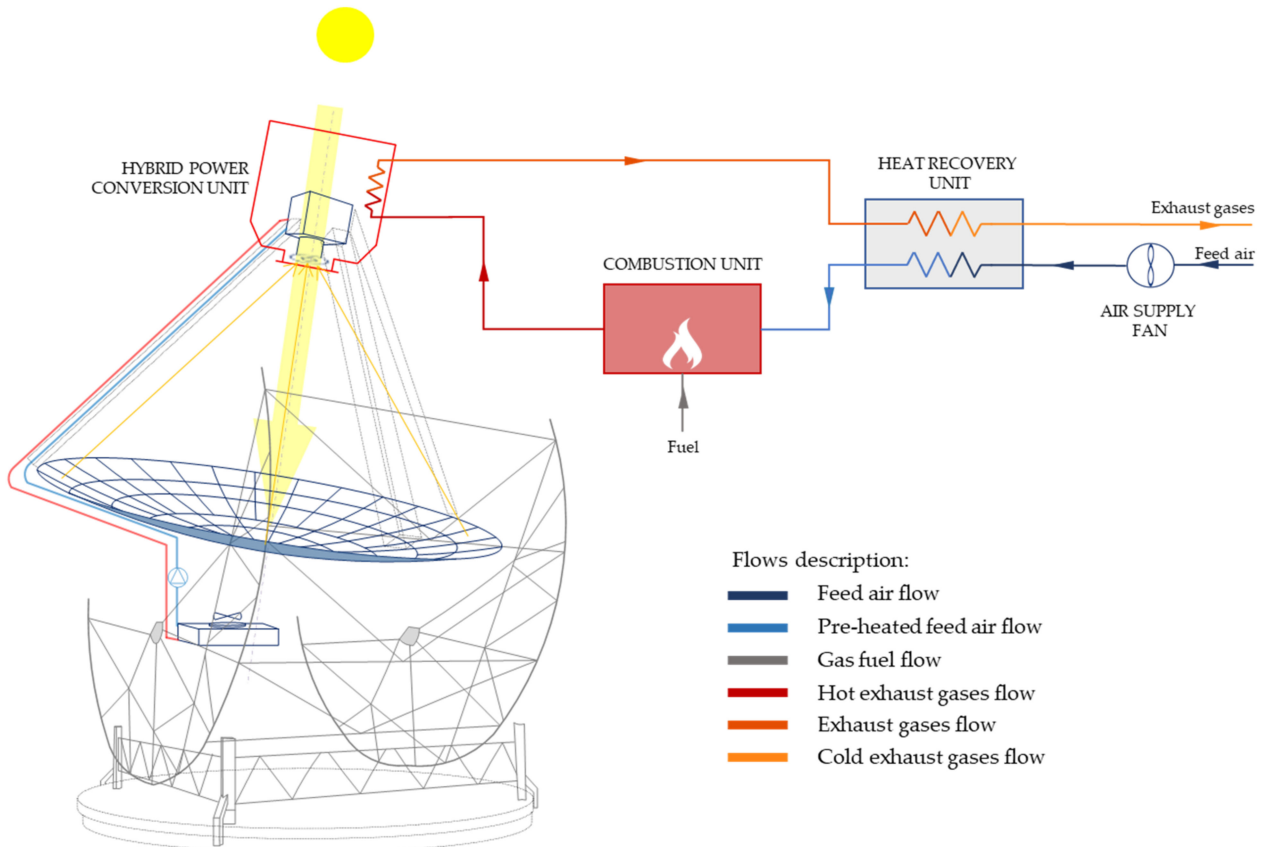


Figure 1. Schematic representation of the plant layout of the hybrid dish-Stirling solar concentrator.

The operation of the hybrid dish-Stirling system (see Figure 1) employs high-temperature gases produced by the oxidation reaction of the fuel gas in the presence of air in the combustion chamber. These gases flow towards the power conversion unit (PCU) providing the high-temperature thermal power required for running the Stirling engine. In this way, the working fluid (hydrogen, air, or helium) reaches its nominal temperature and pressure conditions necessary to evolve inside the Stirling engine and perform the thermodynamic transformations of the homonymous cycle. Downstream of the heat exchange in the PCU, the still hot exhaust gases are sent to a heat recuperator in order to preheat the countercurrent feed airflow.

2.1. Energy Model of a Hybrid Dish-Stirling Concentrating Solar Power Plant

The heart of the hypothesized hybrid solar plant layout is undoubtedly the dish-Stirling solar concentrator, whose engine can be powered by the high-temperature thermal energy obtained from either concentrating solar radiation or the combustion of various types of fuels. In order to assess the energy producibility of the hybrid dish-Stirling system, it is necessary to update the reference energy model of the solar power plant [26], which was calibrated and validated on the basis of experimentally collected data. To this aim, new terms relating to the energy input and losses characterizing the operation of the system in hybrid set-up were added. The reference energy model, based on the energy balance of

the system, approximates the dependence between the mechanical output power (\dot{W}_s) and the thermal input power ($\dot{Q}_{S,in}$) of the engine with a linear correlation, as shown in Equation (1) below:

$$\dot{W}_s = (a_1 \cdot \dot{Q}_{S,in} - a_2) \cdot R_T \quad (1)$$

where a_1 and a_2 are two fitting parameters characterizing the linear correlation, and R_T is an ambient temperature correction factor defined as the ratio between the ambient temperature reference value (set at 25 °C) and the actual temperature, both expressed in Kelvin degrees.

As shown in Figure 2, according to the hybridization hypothesis to be investigated, $\dot{Q}_{S,in}$ represents the engine input thermal power that will be obtained from the available DNI or, alternatively, from the products of gas combustion. In both cases, it is necessary to take into account the upper operating limit of the Stirling engine in terms of the maximum thermal power input to the engine.

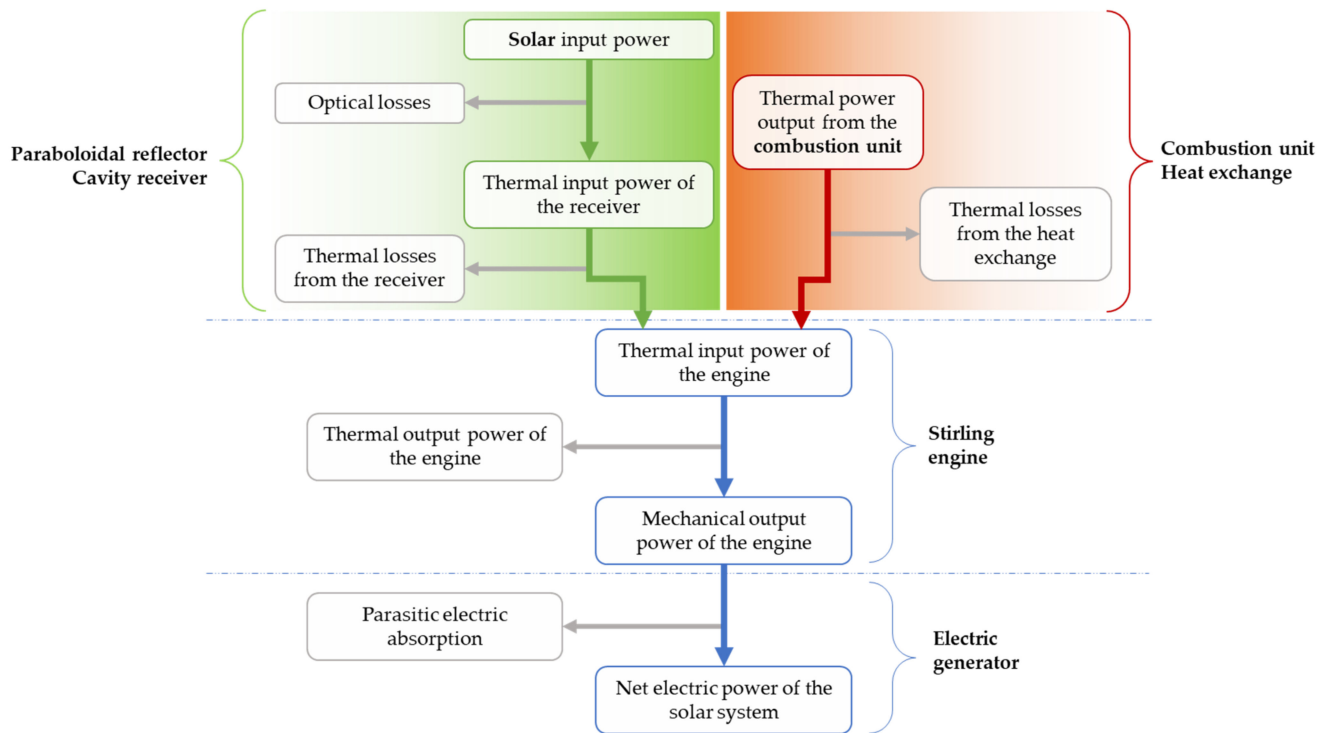


Figure 2. Flow chart of the energy model: solar and non-solar operating mode.

When the dish-Stirling concentrator operates in solar mode (see Figure 2), the thermal power delivered to the Stirling engine ($\dot{Q}_{S,in}^{solar}$) is obtained as the difference between the solar power concentrated at the receiver and the amount of power lost because of thermal and optical inefficiencies. Starting from the paraboloidal reflector, the collected solar power (\dot{Q}_{sun}) is defined as the product of the solar beam radiation (I_b), and the net mirror area (A_n) as described in Equation (2) below:

$$\dot{Q}_{sun} = I_b \cdot A_n \quad (2)$$

Considering the optical inefficiencies of both reflector and receiver surfaces, the power absorbed by the receiver cavity ($\dot{Q}_{r,in}$) can be evaluated as follows:

$$\dot{Q}_{r,in} = \dot{Q}_{sun} \cdot \eta_o \cdot \eta_{cle} = \dot{Q}_{sun} \cdot \rho \cdot \gamma \cdot \alpha \cdot \eta_{cle} \quad (3)$$

where η_{cle} indicates the cleanness level of mirrors, η_o is the optical efficiency of the concentrator obtained as a product of the reflectivity of mirrors (ρ), the intercept factor (γ) which takes into account the tracking errors, the focusing inaccuracy and the wind effect, etc., and the absorption coefficient of the receiver cavity (α). Additionally, due to the differences in temperature between the receiver and the surrounding environment, the receiver energy balance is also affected by thermal losses, which can be divided into convective ($\dot{Q}_{r,conv}$) and radiative thermal losses ($\dot{Q}_{r,rad}$), as defined in the equations below:

$$\dot{Q}_{r,out} = \dot{Q}_{r,conv} + \dot{Q}_{r,rad} \quad (4)$$

$$\dot{Q}_{r,conv} = A_r \cdot h_r \cdot (T_r^{ave} - T_{air}) \quad (4a)$$

$$\dot{Q}_{r,rad} = A_r \cdot \varepsilon_r \cdot \sigma \cdot \left[(T_r^{ave} + 273.15)^4 - (T_{sky} + 273.15)^4 \right] \quad (4b)$$

The following variables are included in these last equations:

- the average temperature of the receiver cavity (T_r^{ave});
- the external air temperature (T_{air});
- the effective sky temperature (T_{sky}) that was derived by the following empirical expression [27–29]:

$$T_{sky} = 0.0552 \cdot (T_{air} + 273.15)^{1.5} - 273.15 \quad (5)$$

- the aperture area of the receiver (A_r);
- the emissivity of the receiver cavity (ε_r); and
- the Stefan–Boltzmann constant (σ).

Finally, the thermal power delivered to the Stirling engine ($\dot{Q}_{S,in}^{solar}$) can be expressed as follows:

$$\dot{Q}_{S,in}^{solar} = \dot{Q}_{r,in} - \dot{Q}_{r,out} \quad (6)$$

$$\dot{Q}_{S,in}^{solar} = I_b \cdot A_n \cdot \eta_o \cdot \eta_{cle} - A_r \cdot \left\{ h_r \cdot (T_r^{ave} - T_{air}) + \varepsilon_r \cdot \sigma \cdot \left[(T_r^{ave} + 273.15)^4 - (T_{sky} + 273.15)^4 \right] \right\} \quad (6a)$$

On the other hand, when the dish-Stirling concentrator is operating in non-solar-mode (see Figure 2), it is assumed that the maximum thermal input power that can be processed by the Stirling engine is obtained through heat exchange with the hot gases coming from the combustion chamber. More specifically, in this case, the thermal power fed into the Stirling engine ($\dot{Q}_{S,in}^{fuel}$) is equal to the nominal thermal power of the combustor reduced by the thermal losses due to its inefficiencies (η_{th}^c) and the heat exchange between the hot gases coming from the combustor and the working fluid of the engine (η_{th}^{ht}). Thus, it is possible to derive the volumetric flow rate of the fuel gas (\dot{V}_{fuel}) supplied to the combustor inlet as follows:

$$\dot{V}_{fuel} = \frac{\dot{Q}_{S,in}^{fuel}}{LHV \cdot \eta_{th}^c \cdot \eta_{th}^{ht}} \quad (7)$$

where LHV is the lower heating value of the used fuel gas.

To summarize, the mechanical power delivered by the engine (defined by Equation (1)) can be recast as follows, depending on the operating mode of the system:

$$\dot{W}_s = (a_1 \cdot \dot{Q}_{S,in} - a_2) \cdot R_T \quad \text{where} \quad \begin{cases} \dot{Q}_{S,in} = \dot{Q}_{S,in}^{solar} & \text{in solar-mode} \\ \dot{Q}_{S,in} = \dot{Q}_{S,in}^{fuel} & \text{in hybrid-mode} \end{cases} \quad (8)$$

For both modes of operation explored, the net electrical power generated by the system under consideration can be defined as the difference between the gross electric output power and the electric power absorbed by the auxiliary components (\dot{E}_p). Among them, the cooling system of the Stirling engine and the solar tracking system were considered. Moreover, taking into account the mechanical-to-electric power conversion efficiency of the electric generator (η_{m-e}), the gross electric output power of the system (\dot{E}_g) can be written as in the following equation:

$$\dot{E}_g = \dot{W}_s \cdot \eta_{m-e} \quad (9)$$

In conclusion, the net electrical power generated by the system (\dot{E}_n) can be defined as follows:

$$\dot{E}_n = \dot{E}_g - \dot{E}_p \quad (10)$$

Therefore, knowing the annual energy producibility of the hybrid system (E_t^{hybrid}) obtained by integrating the instantaneous electric output power of the system (see Equation (10)) over time, the annual generation efficiency of the system (η_G) can be assessed as follows:

$$\eta_G = \frac{E_t^{hybrid}}{Q_{sun} + Q_{fuel}} = \frac{(E_t^{solar} + E_t^{fuel})}{Q_{sun} + Q_{fuel}} \quad (11)$$

where E_t^{solar} and E_t^{fuel} are the annual amounts of electricity produced by solar energy source and fuel, respectively, in the t -th year; and Q_{sun} and Q_{fuel} are the annual energy input to the hybrid dish-Stirling system when it operates in solar mode and non-solar-mode, respectively, during the same year.

In this study, the energy performance of the dish-Stirling system analysed in the hybrid-operating configuration was measured on the basis of the annual electricity production efficiency value calculated as in Equation (11).

2.2. Environmental Analysis

In this study, the environmental analysis of the proposed hybrid dish-Stirling system was carried out by assessing the amount of CO₂ equivalent avoided emissions, as well as the amount of CO₂ that would be emitted annually if the same amount of electricity produced from renewable sources had instead been produced using technologies powered by fossil fuels such as natural gas, oil, or coal. The conversion factor of electricity to CO₂_e emissions depends essentially on two factors, which are the fossil fuel mix typical of the selected country and the categories of technologies for electricity generation that are considered.

Technologies for generating electricity from renewable sources can make a significant contribution to the reduction of greenhouse gas emissions into the atmosphere. Indeed, a life cycle assessment of the various renewable (biopower, photovoltaics, concentrating solar power, geothermal energy, hydropower, ocean energy, and wind energy) and non-renewable electricity generation technologies (nuclear energy, natural gas, oil, and coal) shows that the environmental impact of the former is considerably lower than that of the latter [30]. Specifically, according to the Special Report of the Intergovernmental Panel on Climate Change (IPCC) on Renewable Energy Sources and Climate Change Mitigation

(SRREN), it can be observed that the estimated median values of lifecycle Greenhouse Gases (GHG) emissions for renewable energy technologies do not exceed 0.046 kgCO₂e/kWh with photovoltaics [30]. On the other hand, these median values for technologies fuelled by non-renewable sources reach 0.469, 0.84, and 1.001 kgCO₂e/kWh for natural gas, oil, and coal, respectively [30].

The fossil fuel energy mix of a specific country has been extrapolated from data and statistics published by the International Energy Agency (IEA), which provide the annual electricity generation for each country in the world, from 1990 to 2020, and the share of energy produced from fossil and renewable sources [31].

The amount of equivalent CO₂ avoided emissions (CO₂^{av}), expressed in tonnes per year, was assessed using the following equation:

$$CO_2^{av} = E_t^{renew.} \cdot \mu_{fuel\ mix}^{CO_2} \cdot 10^{-3} \quad (12)$$

where $E_t^{renew.}$ is the total renewable electricity generated by the investigated hybrid power plant during the t -th year (expressed in kWh per year), and $\mu_{fuel\ mix}^{CO_2}$ is the median value of

lifecycle GHG emissions referring to the fossil fuel energy mix (natural gas, oil, coal) that characterized the selected country, expressed in kgCO₂e/kWh.

3. Case Study

This section describes the dish-Stirling plant considered as a reference system and the different case studies investigated for energy and environmental analysis.

3.1. Description of the Reference Dish-Stirling Concentrating Solar Plant

The reference dish-Stirling system is the 31.5 kW_e peak power plant installed at the facility test site on the university campus of Palermo (see Figure 3) in 2017, thanks to the synergy between the Swedish company Ripasso Energy, the manufacturer, and Italian companies Elettrocostruzioni S.r.l. and HorizonFirm S.r.l., who supervised the installation and operational start-up phases.



Figure 3. Dish-Stirling plant installed at the university campus of Palermo.

This grid-connected CSP system is a commercial prototype and consists mainly of a paraboloidal reflector, a bi-axial tracking system, a cavity receiver and a Stirling engine equipped with a cooling system. The main technical features of the dish-Stirling plant in Palermo are reported in Table 1.

Table 1. Main technical parameters characterizing the dish-Stirling concentrator of Palermo.

Parameter	Value	Unit
Aperture area of the receiver (A_r)	0.0314	m ²
Average parasitic electric consumption (\dot{E}_p^{ave})	1600	W
Maximum thermal input power of the engine ($\dot{Q}_{S,in}^{max}$)	84.8·10 ³	W
Clean mirror optical efficiency (η_o)	0.85	-
Convective heat transfer coefficient of the receiver (h_r)	10	W/(m ² ·K)
Emissivity of the receiver (ε_r)	0.88	-
Focal length	7.45	m
Geometric concentration ratio	3217	-
Max operating pressure of hydrogen	200	bar
Mirror cleanliness index (η_{cle})	0.85	-
Net aperture area of the dish collector (A_n)	106	m ²
Parameter a_1 in Equation (1)	0.475	-
Parameter a_2 in Equation (1)	3318.66	W
Reference temperature (T_0)	25	°C
Reflectivity of clean mirror (ρ)	0.95	-
Temperature of the receiver (T_r^{ave})	720	°C

More specifically, the paraboloidal reflector has a diameter of 11.86 m and consists of an assembly of 104 highly reflective mirrors of different shapes. Each of these mirrors has a double curvature and concentrates the solar beam radiation at a focal point where, at a focal length of 7.45 m, the aperture of the cavity receiver is fixed. The fundamentals of this solar technology require the perfect alignment between the axis of the paraboloidal concentrator and the direction of sunlight throughout the day. For this purpose, the biaxial tracking system, driven by two motors, continuously modifies the position of the concentrator by matching its azimuth and elevation angles with the position of the sun throughout the day. The solar energy concentrated on the receiver is absorbed within the cavity and then transferred to the evolving fluid, hydrogen. The use of hydrogen, characterized by a lower dynamic viscosity than air or helium at operating temperatures [32], ensures the good mechanical performance of the Stirling engine due to reduced dynamic fluid friction losses. In this way, the hydrogen reaches the nominal pressure and temperature conditions of 200 bar and 720 °C.

The solar Stirling engine of the reference solar plant has four double-action cylinders with regenerators and can elaborate a maximum thermal input power of 84.8 kW, which can be achieved with clean mirrors, normal direct irradiance of 960 W/m² and external air temperature of 25 °C. At these operating conditions, this Stirling engine can achieve thermal efficiency values of over 40% [26].

While the receiver continuously supplies high-enthalpy thermal energy to the hot side of the engine, the cooling system keeps the cold side of the engine at a temperature of approximately 70 °C by dissipating the waste heat into the environment using a dry-cooler fixed to the back of the reflector. The plant has a total weight of 8000 kg and occupies a total area of 500 m².

3.2. Description of the Investigated Case Studies

The investigated hybrid plant layout integrates the dish-Stirling solar concentrator with a system that includes the combustion unit, the combustion feed system, and the heat exchange between hot gases from combustion and hydrogen. The latter system was considered as a black box with an overall efficiency of 80%.

Based on the previous section, two modes of operation have been defined for the proposed hybrid plant layout: a solar mode, if it is powered by a solar source only; and a non-solar mode, if it is powered by heat obtained through gas combustion. Different scenarios of operation of the hybrid system have been investigated, which are:

- Scenario 0, according to which the examined system operates exclusively in solar mode.
- Scenario I, according to which the dish-Stirling system operates in solar mode during daylight hours and in non-solar mode from 7 p.m. to midnight.
- Scenario II, according to which the dish-Stirling system operates in solar mode during daylight hours and in non-solar mode from 7 p.m. to 4 a.m. the next day.
- Scenario III, according to which the dish-Stirling system operates in solar mode during daylight hours and in non-solar mode from 7 p.m. to 7 a.m. the next day, in order to allow 24-h operation at least on clear days of the year.

In addition, each of these above-mentioned scenarios was investigated by considering the following alternatives:

- three potential installation sites located in the Sunbelt region [33] and characterized by different levels of direct normal irradiation (see Table 2):
 1. Palermo (Italy), the capital of Sicily (a region in Southern Italy), where the reference dish-Stirling solar plant is installed.
 2. Abu Dhabi (United Arab Emirates), and more precisely the same location to the west of this capital city that hosts Shams, which is the largest renewable energy project in operation in the Middle East. This solar field has 768 parabolic collectors to generate clean, renewable electricity and has a capacity of 100 MW [24].
 3. The Mojave Desert (California, United States), and more precisely the same location at which the Mojave Solar Project (MSP) is installed. This project consists of two solar fields for a total power capacity of 250 MW and uses parabolic trough CSP technology [25].
- three different fuel gases to burn in the combustion unit (see Table 3):
 1. natural gas;
 2. biogas; and
 3. syngas.

Table 2. Geographic coordinates and direct normal irradiation (DNI) level of selected locations.

Location	Geographical Coordinates and Elevation [m]	Direct Normal Irradiation [kWh/(m ² ·Year)]
Palermo ¹	38.1° N 13.4° E—50	1804.9
Abu Dhabi ¹	23.6° N 53.7° E—130	2207.9
Mojave Desert ²	34.9° N 117.3° E—635	2996.3

¹ Data extrapolated from Typical Meteorological Year (TMY) (period: 2005–2020) provided by the PVGIS-SARAH2 solar database. ² Data extrapolated from TMY (period: 2005–2015) provided by the PVGIS-NSRDB solar database [34,35].

Table 3. Lower heating value (LHV) of selected fuel gases.

Fuel Gas	LHV [MJ/kg]
Natural gas	35
Biogas	23
Syngas	5

3.2.1. Potential Installation Sites Investigated for the Proposed Hybrid System

As described in Section 2.1 on the energy balance of dish-Stirling systems, the climate factors that influence the electrical producibility are the DNI and, marginally, the external air

temperature. The former drives the input power to the system, while the latter characterizes the thermal losses at the receiver [26]. By discretizing the data extrapolated from the TMYs provided by the PVGIS-SARAH2 solar database [36] for Palermo and Abu Dhabi, and from the TMY provided by PVGIS-NSRDB solar database [35] for the Mojave Desert, it was possible to obtain the hourly-frequency distribution of the DNI for classes with a width of 50 W/m^2 [37] and the corresponding mean value of the external air temperature (see Figure 4).

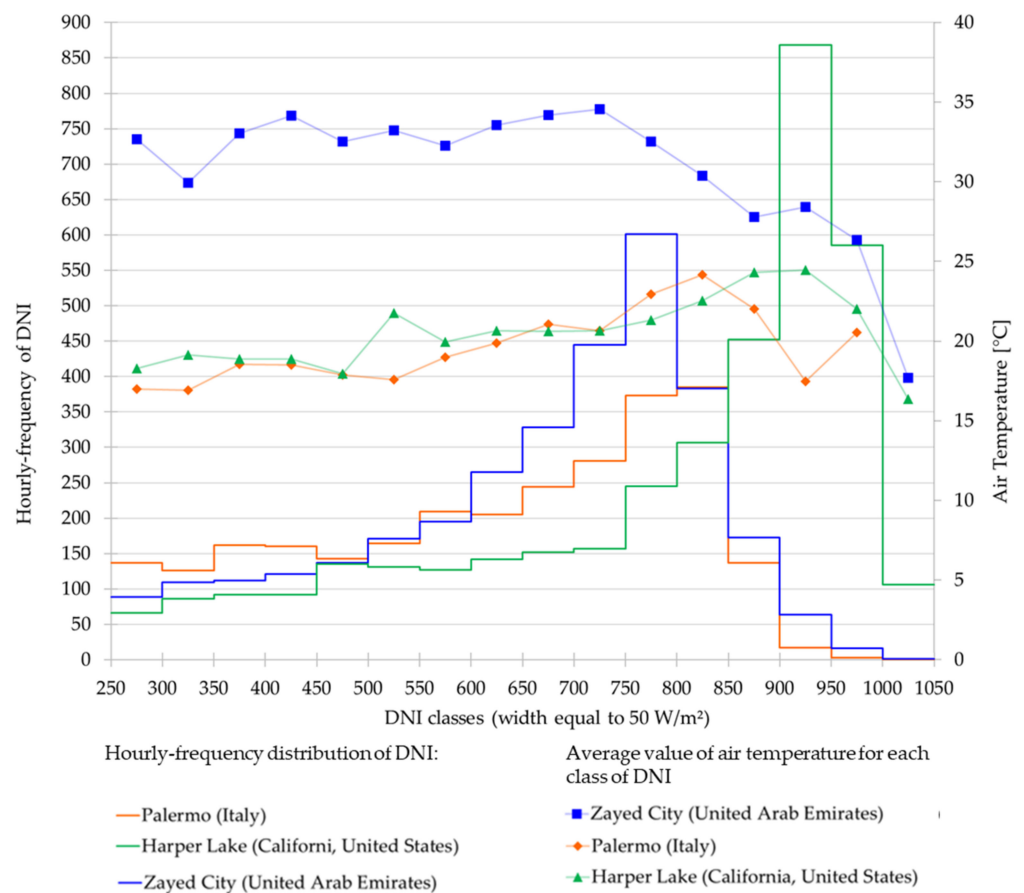


Figure 4. Hourly-frequency distributions of the DNI (step plots) and average values of the external air temperature for each class of DNI (connected scatterplots) referring to all selected locations: Palermo, Abu Dhabi and the Mojave Desert.

Observing Figure 4, it can be noted that:

- The three selected locations have hourly DNI distributions with peaks falling into quite different DNI classes: the distribution of DNI for Palermo presents a peak of 385 h per year falling in the DNI class between 800 and 850 W/m^2 ; the one for Abu Dhabi presents a higher peak of 601 h per year falling in the DNI class between 750 and 800 W/m^2 ; and finally, the one for the Mojave Desert presents the highest peak of 868 h per year falling in the DNI class between 900 and 950 W/m^2 .
- For DNI classes from 250 to 600 W/m^2 , Palermo always has a higher hourly frequency value than the other two locations.
- In Palermo, the number of hours in which a DNI between 900 and 1000 W/m^2 occurs is small compared to that characteristic of Abu Dhabi, and considerably less than the Mojave Desert.

Comparing the hourly-frequency distributions of DNI for Abu Dhabi and Palermo, it can be seen that the former, despite the prevalence of clear sky days during the year, peaks in a lower class than the latter due to the particular climatic conditions that characterize the

region, which includes the Middle East and North Africa. Indeed, these geographical areas, being desert and arid, are characterized by significant concentrations of aerosols in the atmosphere which cause the attenuation of the normal component of solar radiation that arrives on the Earth's surface [38]. On the other hand, the lower concentration of aerosols in the atmosphere typical of Europe combined with the lower aerosol optical depth (AOD) has a weaker attenuation effect on the intensity of the DNI, producing a brightening effect [39].

Concerning the outside air temperatures, Figure 4 shows the average outside air temperature values corresponding to each DNI class, and Figure 5 shows the average daily values of outside air temperature for the three locations examined. The following can be noted:

- As Figure 4 shows, there is a correspondence between the peak DNI hourly-frequency distribution and the maximum temperature. This indicates that clear days mainly occur during the warmer months of the year. Conversely, the fact that higher DNI classes have lower average temperatures results from the possibility that clear sky days occur during the colder months of the year, although they are less prevalent.
- Figure 5 shows that Abu Dhabi is the warmest location throughout the year compared to the other two studied locations. The average daily temperatures range between 13.7 and 39.4 °C in Abu Dhabi, between about 3 and 33.3 °C in the Mojave Desert location, and between 3 and 29.9 °C in Palermo.

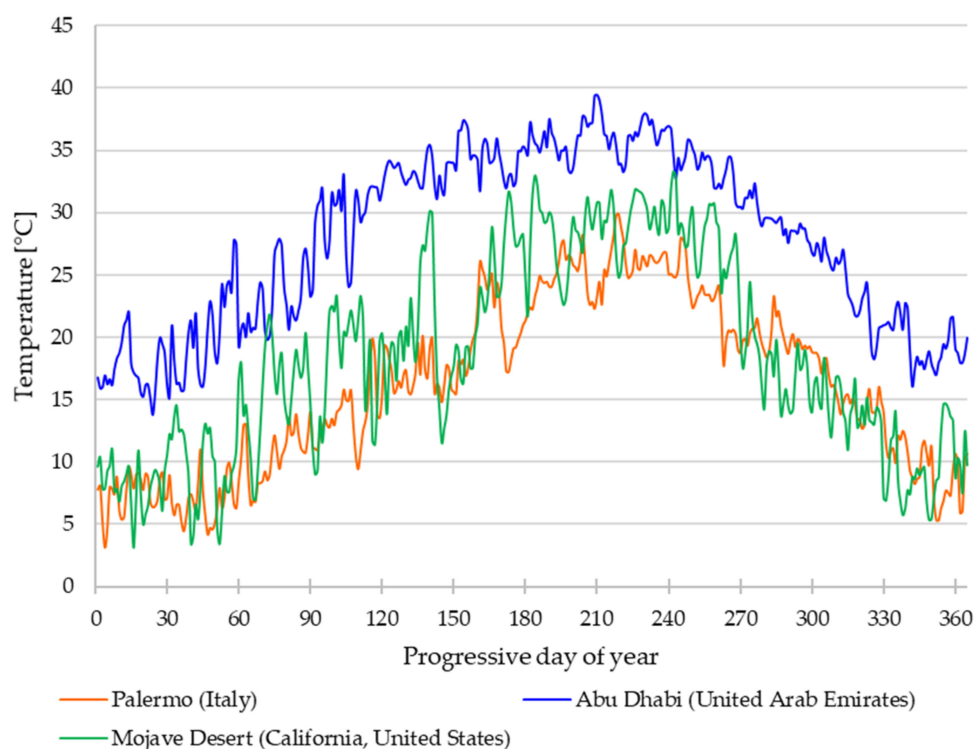


Figure 5. Daily average values of the external air temperature for all selected locations: Palermo, Abu Dhabi, and the Mojave Desert.

Furthermore, in order to be able to estimate the annually avoided equivalent CO₂ emissions, according to Section 2.2, the fossil fuel energy mix and lifecycle GHG emissions for the countries of the three selected locations were deduced from the electricity data provided by the IEA [31]. These data are reported in Table 4 and refer to 2019, as these are the most recent but also the most comprehensive for all countries of interest.

Table 4. Electricity data provided by the IEA [31] and derived quantities for 2019: fossil fuel energy mix and lifecycle GHG emissions deduced for selected countries.

	Italy	United Arab Emirates	United States
Total energy production [GWh]	293,853	138,454	4,391,761
Energy production from fossil fuel [GWh]	173,093	134,675	2,745,142
Fossil Fuel Energy Mix [%]:			
1. Natural gas	81.9	99.4	59.7
2. Oil	5.9	0.6	1.3
3. Coal	12.3	0.0	39.0
$\mu_{fuel}^{CO_2}$ [kgCO ₂ e/kWh] <i>mix</i>	0.546	0.462	0.675

3.2.2. Fuel Alternatives to Power the Proposed Hybrid System

The operation of the hybrid dish-Stirling system proposed in this work was investigated, assuming that the combustion unit could be supplied with natural gas, syngas, or biogas. These fuels are briefly described in the following.

Natural gas is a non-renewable energy source that, like oil, is formed by a geological process of crushing and decomposing organic matter deep underground and near the hot earth's core. Indeed, the formation of light hydrocarbons such as natural gas requires high temperatures and pressures [40]. Natural gas has a chemical composition that varies depending on the geographic location where it is extracted, but it generally consists mainly of methane (CH₄), with up to 20% propane (C₃ H₈) and ethane (C₂ H₆) [41]. It is colourless and odourless, and must be injected with a mercaptan, so that any leakage can be detected by smell. Natural gas is considered to be the cleanest fossil fuel for energy production, being the fossil fuel with the lowest environmental impact compared to other commonly used fuels. The CO₂ emissions due to the use of natural gas are 40–50% and 25–30% lower than those of coal and fuel oil, respectively [42]. With regard to thermal capacity, for natural gas, a lower heating value (LHV) of 35 MJ/Nm³ was assumed (see Table 3).

Syngas has traditionally been derived from fossil fuels, but alternatively, it can be produced by biomass gasification, water electrolysis, or electrocatalytic reduction of CO₂, and depending on the production process, the composition of the resulting syngas can change considerably [43]. Syngas is the main product obtained through the gasification of non-renewable and renewable energy sources such as coal and lignocellulosic biomass, respectively. This process is defined as the thermochemical conversion of carbonaceous materials in a partially oxidised environment to produce coal, tar and a gas mixture consisting of carbon monoxide, hydrogen, carbon dioxide, and methane, as well as other low molecular weight hydrocarbons [44]. Lignocellulosic biomass, as a renewable source, has great potential to be used as the main raw material to produce syngas by gasification, thus decreasing the exploitation of coal. Air, oxygen, and steam are the main oxidizing agents used to perform gasification and, for each of them, the syngas obtained is characterised by different heating values due to the variation of the H₂ and CO concentration. Air is one of the most used gasification media because it has no costs associated with its purchase and use. However, the syngas produced by air gasification has the lowest heating value that can be obtained through this technology. This is due to the presence of N₂ and other impurities in the composition of the syngas [45]. Thus, syngas obtained from gasification of lignocellulosic biomass as the raw material with an air oxidising agent has a high heating value (HHV) ranging between 4 and 7 MJ /Nm³, with an H₂ content between 12 and 16%, a CO content of 18–24%, and a CH₄ content of 1–6% [46]. By replacing air with oxygen or water vapour, it is possible to obtain syngas with HHV values of 10–18 MJ/Nm³ and 12–28 MJ/Nm³, respectively, being free of N₂ and with a high H₂ and CO content [47].

In this study, syngas has been considered a renewable alternative to natural gas as it could be obtained from lignocellulosic biomass from virgin biomass, energy crops or

agricultural waste [48]. An LHV equal to 5 MJ/Nm³ has been assumed [49] (see Table 3) and a null CO₂ conversion factor since carbon dioxide released from the use of syngas is balanced by the sequestration of carbon dioxide by plants during photosynthesis.

Biogas is the main product obtained from the anaerobic digestion of organic matter or biomass. This process is a complex sequence of chemical reactions in which organic matter is degraded and stabilized by the metabolic activity of microorganisms in an oxygen-free environment. The main product of the digestion process is a gas mixture consisting mainly of methane (CH₄) and carbon dioxide (CO₂), and traces of hydrogen sulphide (H₂S), ammonia (NH₃), hydrogen (H₂) and carbon monoxide (CO). Lignocellulosic biomass is an abundant renewable resource that can be used for biogas production, being a potential source of fermentable sugars such as glucose, xylose, mannose and arabinose, as well as other organic compounds such as proteins and lipids that can be degraded anaerobically [45]. Depending on its origin, biogas is usually characterised by 55–70% methane, 30–45% carbon dioxide, and traces of other gases [42], and energy content ranging between 19 and 26 MJ/m³ [47]. Once the biogas has been produced, it can be cleaned or upgraded (through absorption, adsorption, membrane separation, and cryogenic separation) to increase its heating value according to the application for which it is intended.

Thus, in this study, as a second alternative to natural gas, it is supposed that biogas obtained by anaerobic digestion of lignocellulosic biomass is used, assuming an LHV equal to 23 MJ/Nm³ [42] (see Table 3). In addition, in this case, the null CO₂ conversion factor has been considered.

Unlike natural gas, which is more widely available and an easily accessible resource, the use of biogas or syngas in distributed power generation plants, such as the one proposed, requires the on-site installation of biomass treatment facilities, since renewable fuel distribution networks are not yet widespread [42]. This study aims to investigate the energy and environmental performance of the hybrid dish-Stirling system for the different scenarios illustrated and it is assumed that the quantity of the fuel gases considered, renewable or fossil, required by the hybrid plant hypothesis are available.

4. Results and Discussion

In accordance with the energy model described and detailed in Section 2.1, it was possible to estimate the electrical energy production of the investigated hybrid dish-Stirling system in both solar and non-solar operating modes. Table 5 shows the annual electricity productions that were evaluated for all the considered scenarios: the electricity production indicated for Scenario 0 (E_t^{solar}) is calculated considering the system operating always and only in solar operation mode, while the electricity production indicated for Scenarios I, II, and III is strictly related to the period in which the same system operates in non-solar mode (E_t^{fuel}). Therefore, to these latter quantities (E_t^{fuel}), the production from solar sources (E_t^{solar}) must be added to obtain the total annual production of the hybrid system (E_t^{hybrid}).

Table 5. Annual electricity generation of the hybrid dish-Stirling system investigated.

E_t [MWh]	Palermo	Abu Dhabi	Mojave Desert
Scenario 0 (E_t^{solar})	43.7	53.1	79.7
Scenario I (E_t^{fuel})	73.1	70.7	71.1
Scenario II (E_t^{fuel})	122.0	118.4	118.5
Scenario III (E_t^{fuel})	158.8	153.6	154.6

From Table 5, it can be observed that electricity production evaluated for Scenario 0 clearly increases by considering Palermo, Abu Dhabi and the Mojave Desert, in that order,

as they are characterized by progressively higher levels of DNI (see Scenario 0 in Table 5). On the other hand, the electricity generated by the combustion of fuel does not reflect this same trend as the location varies. Indeed, the conversion efficiency of the Stirling engine is affected by the effectiveness of the heat exchange with the environment on the cold side, and this is worse in Abu Dhabi, being the warmest location (see Figure 5). Specifically in Palermo, annual simulations show that the hybridization of the dish-Stirling system would increase solar electricity production by 63%, 74%, and 78% for scenarios I, II, and III, respectively.

Furthermore, from Table 6, which shows the generation efficiency values calculated in accordance with Equation (11), it emerges that the increase in annual electricity production of the hybrid system would also be accompanied by an improvement in its generation efficiency, which is greater the longer the period of non-solar operation of the system (it becomes maximum for Scenario III).

Table 6. The annual generation efficiency of the investigated hybrid dish-Stirling system.

η_G [%]	Palermo	Abu Dhabi	Mojave Desert
Scenario 0	32.7	32.5	35.7
Scenario I	36.8	35.6	37.0
Scenario II	37.6	36.5	37.4
Scenario III	38.0	36.8	37.7

Concerning the operation of the dish-Stirling system in solar mode (Scenario 0), the results obtained from the annual simulations show that the system could achieve an annual generation efficiency of 35.7% if it was installed at the Mojave Desert location. This efficiency value is higher than those obtained for the other two installation locations investigated. This result is supported by the fact that, from the hourly-frequency distribution of DNI for the Mojave Desert on an annual basis (see Figure 4), approximately 50% of the hours with DNI greater than 250 W/m² fall within the DNI range between 850 and 1000 W/m², and of these, approximately 45% of the hours correspond to DNI values between 900 and 950 W/m². This would mean that if the dish-Stirling pilot plant installed in Palermo, having been sized for a nominal DNI level of 960 W/m², was installed in the Mojave Desert, it could exhibit the best conversion efficiency when operating in solar mode, achieving a generation efficiency on an annual basis of 35.7.

Tables 7–9 below show results obtained from the environmental analysis in terms of avoided CO₂ equivalent emissions expressed in tons per year, as explained in Section 2.2 above. To this aim, the median value of lifecycle GHG emissions referring to the fossil fuel energy mix of each selected country was used (see Table 4).

Table 7. The annual amount of avoided equivalent CO₂ emissions associated with the electricity production of the dish-Stirling system operating in solar mode.

CO ₂ ^{av} [ton/year]	Palermo	Abu Dhabi	Mojave Desert
Scenario 0	23.9	24.5	53.8

Table 8. The annual amount of avoided equivalent CO₂ emissions associated with the electricity production of the dish-Stirling system operating in non-solar mode (powered by biogas or syngas).

CO ₂ ^{av} [ton/year]	Palermo	Abu Dhabi	Mojave Desert
Scenario I	39.9	32.6	47.9
Scenario II	66.6	54.6	79.9
Scenario III	86.7	70.9	104.3

Table 9. The annual amount of avoided equivalent CO₂ emissions associated with the electricity production of the dish-Stirling system operating in non-solar mode (powered by natural gas).

CO ₂ ^{av} [ton/year]	Palermo	Abu Dhabi	Mojave Desert
Scenario I	6.3	0.1	15.3
Scenario II	10.5	0.2	25.4
Scenario III	13.7	0.3	33.2

Specifically, Table 7 shows the equivalent avoided CO₂ emissions (CO₂^{av}) that could be achieved through the generation of renewable electricity by the dish-Stirling system operating in solar mode. From these results, it can be seen that the expected environmental benefits change significantly depending on the assumed location of the renewable energy plant, because the energy mix on which each country's energy production is based differs. Of the three possible locations considered, the avoided CO₂ equivalent emissions would be higher if the dish-Stirling system were installed in the Mojave Desert, as coal currently accounts for 39% of total electricity production in the United States.

Furthermore, referring to the hybrid dish Stirling system fed with syngas or biogas, the avoided quantities of CO₂ equivalent emissions obtained for Scenario 0 (see Table 7) should be increased by the quantities calculated for Scenarios I, II and III (see Table 8). Indeed, in this case, the dish Stirling would operate in hybrid mode using not only the solar source, but also heat obtained from the combustion of syngas or biogas, which can be considered renewable and CO₂-neutral if derived from lignocellulosic biomass.

It would be different if the Stirling engine in the hybrid configuration were powered by natural gas instead of biogas or syngas. In this case, the CO₂ avoided emissions were evaluated as the difference between those calculated considering the emission factor characteristic of the country of interest and those calculated considering the emission factor related to the use of only natural gas. These results are reported in the following table.

5. Conclusions

There are several theoretical and experimental studies published in the literature on hybrid dish-Stirling systems, and all of these demonstrate and validate its technological feasibility. In this paper, a study was carried out on a commercial prototype dish-Stirling system with a size of 31.5 kW_e, which holds the world record for solar-to-electric energy conversion efficiency, making the Ripasso dish-Stirling system a state-of-the-art system in the CSP sector. Therefore, before proceeding to the design and then to the executive phase, in this study, the energy and environmental benefits that would be possible through the operation of such dish-Stirling system in hybrid set-up also in different locations around the world that already host important CSP projects have been evaluated and verified. The following considerations can be made after this study.

- This study further proves the influence of climatic factors typical of the installation location on the electrical output of the dish-Stirling, whether from solar or non-solar sources. Indeed, by observing the results of the electricity production related to the solar mode of operation, it is possible to appreciate the prevalent influence of DNI on production. The annual production of the dish-Stirling is gradually increasing, considering Palermo, Abu Dhabi and the Mojave Desert, in that order, being equal to 43.7, 53.1, and 79.7 MWh, respectively. On the other hand, it is possible to appreciate the minor influence of the external air temperature on the energy performance of the examined system by observing the annual electricity productions obtained, considering only the hours in which the system is operated by a non-solar source. These are higher for Palermo even if only slightly compared to the other two locations since it is the one with lower average external air temperatures throughout the year. These considerations have an impact also in terms of annual generation efficiency.
- The environmental analysis and, therefore, the evaluation of the avoided equivalent CO₂ emissions deriving from the production of electrical energy from renewable

sources has been carried out considering the technological context and the mix of fossil fuels typical of the country of interest for the hypothetical site of installation. Considering a useful life of the plant of 25 years, it would be possible to produce electricity from solar sources avoiding the emission of an amount of equivalent CO₂ equal to 597.5, and 612.5, and 1345 tons in Italy, the United Arab Emirates, and the United States, respectively. The greatest environmental benefits for the same electricity production would be in the United States, where coal accounts for approximately 40% of the fossil fuel mix in electricity generation. For this reason, the installation of dish-Stirling systems could be more favourable. If the dish-Stirling system were hybridized by exploiting the thermal potential of biogas or syngas derived from lignocellulosic biomass, these benefits would be greatly increased by being able to consider these gases renewable fuels with a zero-carbon cycle.

An economic analysis of the hybrid system proposed here and its relative effect on the levelized cost of energy will be conducted in a future study.

Author Contributions: Conceptualization, S.G. and A.B.; methodology, S.G.; software, S.G. and A.B.; validation, S.G.; formal analysis, S.G.; investigation, S.G.; writing—original draft preparation, S.G. and A.B.; writing—review and editing, S.G. and A.B.; supervision, V.L.B. and A.M. All authors have read and agreed to the published version of the manuscript.

Funding: This research received no external funding.

Institutional Review Board Statement: Not applicable.

Informed Consent Statement: Not applicable.

Acknowledgments: The authors express gratitude to the companies HorizonFirm S.r.l, Christian Chiaruzzi, Elettrocostruzioni S.r.l. and Ripasso Energy for the support provided, without which it would not have been possible to install the dish-Stirling concentrator plant on the Palermo university campus.

Conflicts of Interest: The authors declare no conflict of interest.

Nomenclature

Symbols

a_1	fitting parameter characterizing the linear energy model [–]
a_2	fitting parameter characterizing the linear energy model [W]
A_n	net mirrors area [m ²]
A_r	the aperture area of the receiver [m ²]
CO ₂ ^{av}	the amount of equivalent CO ₂ emissions avoided [tons/year]
\dot{E}_g	the gross electric power output of the system [W]
\dot{E}_p	the parasitic electrical power absorbed by the auxiliary components [W]
\dot{E}_p^{ave}	the average electrical power absorbed by the auxiliary components [W]
\dot{E}_n	the net electrical power generated by the system [W]
E_t^{fuel}	the annual electricity produced by the system operating in non-solar-mode [MWh]
E_t^{hybrid}	the annual energy producibility of the hybrid system [MWh]
$E_t^{renew.}$	the total renewable electricity generated by the hybrid power plant [MWh]
E_t^{solar}	the annual electricity produced by the system operating in solar-mode [MWh]
h_r	the convective heat transfer coefficient of the receiver [W/(m ² ·K)]
I_b	solar beam radiation [W/m ²]
LHV	lower heating value [MJ/kg]
Q_{fuel}	the annual input energy of the hybrid dish-Stirling system operating in non-solar mode [MWh]
$\dot{Q}_{r,conv}$	convective thermal losses affecting the receiver [W]
$\dot{Q}_{r,in}$	absorbed power by the receiver cavity [W]
$\dot{Q}_{r,out}$	thermal output power of the receiver [W]

$\dot{Q}_{r,rad}$	radiative thermal losses affecting the receiver [W]
$\dot{Q}_{S,in}$	thermal input power of the Stirling engine [W]
$\dot{Q}_{S,in}^{max}$	maximum thermal input power of the Stirling engine [W]
$\dot{Q}_{S,in}^{fuel}$	thermal power input to the Stirling engine operating in non-solar mode [W]
$\dot{Q}_{S,in}^{solar}$	thermal power delivered to the Stirling engine operating in solar mode [W]
\dot{Q}_{sun}	solar power collected by the paraboloidal reflector [W]
Q_{sun}	the annual input energy of the hybrid dish-Stirling system operating in solar-mode [MWh]
R_T	ambient temperature correction factor [–]
T_{air}	the external air temperature [K]
T_r^{ave}	the average temperature of the receiver cavity [K]
T_{sky}	the effective sky temperature [K]
\dot{V}_{fuel}	the volumetric flow rate of the fuel gas [m ³ /s]
\dot{W}_s	mechanical output power of the Stirling engine [W]
Greek letters	
α	the absorption coefficient of the receiver cavity [–]
γ	the intercept factor [–]
ε_r	the emissivity of the receiver cavity
η_{cle}	cleanness level of mirrors [–]
η_G	the annual generation efficiency of the system
η_o	optical efficiency of the concentrator [–]
η_{m-e}	the mechanical-to-electric power conversion efficiency of the electric generator [%]
η_{th}^c	the thermal efficiency of the combustor
η_{th}^{ht}	the efficiency of the heat exchange between the hot gases from the combustion unit and the working fluid of the engine [–]
ρ	the reflectivity of mirrors [–]
σ	the Stefan–Boltzmann constant [W/(m ² ·K ⁴)]
$\mu_{fuel}^{CO_2 mix}$	the median value of lifecycle GHG emissions referred to the fossil fuel energy mix [kgCO _{2e} /kWh]
Abbreviations	
AOD	Aerosol Optical Depth
CSP	Concentrating Solar Power
CO ₂	Carbon Dioxide
DNI	Direct Normal Irradiance
GHG	Greenhouse Gases
IEA	International Energy Agency
IPCC	Intergovernmental Panel on Climate Change
MSP	Mojave Solar Project
PCU	Power Conversion Unit
SRREN	Special Report on Renewable Energy Sources and Climate Change Mitigation
TMY	Typical Meteorological Year

References

1. IEA. *Renewable Power*; IEA: Paris, France, 2021.
2. IRENA. *Renewable Capacity Statistics 2021*; International Renewable Energy Agency (IRENA): Masdar City, Abu Dhabi, 2021.
3. Santos, J.J.C.S.; Palacio, J.C.E.; Reyes, A.M.M.; Carvalho, M.; Freire, A.J.R.; Barone, M.A. Concentrating Solar Power. *Adv. Renew. Energ. Power Technol.* **2018**, *1*, 373–402. [[CrossRef](#)]
4. Wang, Z. The Solar Resource and Meteorological Parameters. *Des. Sol. Therm. Power Plants* **2019**, 47–115. [[CrossRef](#)]

5. Van Sark, W.; Corona, B. Concentrating solar power. In *Technological Learning in the Transition to a Low-Carbon Energy System: Conceptual Issues, Empirical Findings, and Use, in Energy Modeling*; Academic Press: Cambridge, MA, USA, 2020; pp. 221–231. [[CrossRef](#)]
6. Lovegrove, K.; Stein, W. *Concentrating Solar Power Technology: Principles, Developments and Applications*. Woodhead Publishing: Sawston, UK, 2012; ISBN 9781845697693.
7. Guarino, S.; Buscemi, A.; Ciulla, G.; Bonomolo, M.; Lo Brano, V. A dish-stirling solar concentrator coupled to a seasonal thermal energy storage system in the southern mediterranean basin: A cogenerative layout hypothesis. *Energy Convers. Manag.* **2020**, *222*, 113228. [[CrossRef](#)]
8. Sharma, A.; Shukla, S.K.; Rai, A.K. Finite time thermodynamic analysis and optimization of solar-dish Stirling heat engine with regenerative losses. *Therm. Sci.* **2011**, *15*, 995–1009. [[CrossRef](#)]
9. Thombare, D.G.; Verma, S.K. Technological development in the Stirling cycle engines. *Renew. Sustain. Energy Rev.* **2008**, *12*, 1–38. [[CrossRef](#)]
10. Mancini, T.; Heller, P.; Butler, B.; Osborn, B.; Schiel, W.; Goldberg, V.; Buck, R.; Diver, R.; Andraka, C.; Moreno, J. Dish-stirling systems: An overview of development and status. *J. Sol. Energy Eng. Trans. ASME* **2003**, *125*, 135–151. [[CrossRef](#)]
11. Coventry, J.; Andraka, C. Dish systems for CSP. *Sol. Energy* **2017**, *152*, 140–170. [[CrossRef](#)]
12. IRENA. *Renewable Power Generation Costs in 2020*; International Renewable Energy Agency (IRENA): Masdar City, Abu Dhabi, 2020.
13. Singh, U.R.; Kumar, A. Review on solar Stirling engine: Development and performance. *Therm. Sci. Eng. Prog.* **2018**, *8*, 244–256. [[CrossRef](#)]
14. Kumar, D.; Agrawal, M. A Review on Development and Applications of Solar Dish Stirling System. In *Advancement in Materials, Manufacturing and Energy Engineering*; Springer: Berlin/Heidelberg, Germany, 2022; Volume II, pp. 57–70.
15. Malik, M.Z.; Shaikh, P.H.; Zhang, S.; Lashari, A.A.; Leghari, Z.H.; Baloch, M.H.; Memon, Z.A.; Caiming, C. A review on design parameters and specifications of parabolic solar dish Stirling systems and their applications. *Energy Rep.* **2022**, *8*, 4128–4154. [[CrossRef](#)]
16. Bravo, Y.; Monné, C.; Bernal, N.; Carvalho, M.; Moreno, F.; Muñoz, M. Hybridization of solar dish-stirling technology: Analysis and design. *Environ. Prog. Sustain. Energy* **2014**, *33*, 1459–1466. [[CrossRef](#)]
17. Monné, C.; Bravo, Y.; Moreno, F.; Munoz, M. Analysis of a solar dish-Stirling system with hybridization and thermal storage. *Int. J. Energy Environ. Eng.* **2014**, *5*, 80. [[CrossRef](#)]
18. Hartenstine, J.; Dussinger, P. Development of a solar and gas-fired heat pipe receiver for the Cummins power generation 7.5 kWe dish/Stirling system. In *Proceedings of the Intersociety Energy Conversion Engineering Conference, Monterey, CA, USA, 7–12 August 1994*; p. 3864.
19. Blázquez, R.; Carballo, J.; Silva, M. Optical design and optimization of parabolic dish solar concentrator with a cavity hybrid receiver. *AIP Conf. Proc.* **2016**, *1734*, 70002. [[CrossRef](#)]
20. Barbosa, D.; André, P.; Antunes, P.; Paixão, T.; Marques, C.; van Ardenne, A.; Kant, D.; Ebbendorf, N.; Gonzalez, L.S.; Rubio, D.; et al. BIOSTIRLING-4SKA: A cost effective and efficient approach for a new generation of solar dish-Stirling plants based on storage and hybridization; An Energy demo project for Large Scale Infrastructures. *arXiv* **2017**, arXiv:1712.03029.
21. Kang, M.; Kim, J.; Kang, Y.; Kim, N.; Yoo, S.; Kim, J. An experimental study on the heat transfer characteristics of the hybrid solar receiver for a dish concentrating system. In *Proceedings of the ISES World Congress 2007*; Springer: Cham, Switzerland, 2008; Volume I–V, pp. 689–693.
22. Laing, D.; Pálsson, M. Hybrid dish/Stirling systems: Combustor and heat pipe receiver development. *J. Sol. Energy Eng.* **2002**, *124*, 176–181. [[CrossRef](#)]
23. Moreno, J.; Rawlinson, S.; Andraka, C.; Mehos, M.; Bohn, M.S.; Corey, J. Dish/Stirling Hybrid-Receiver Sub-Scale Tests and Full-Scale Design. SAE Technical Paper. 1999. Available online: <https://www.sae.org/publications/technical-papers/content/1999-01-2561/> (accessed on 1 April 2022).
24. Alobaidli, A.; Sanz, B.; Behnke, K.; Witt, T.; Viereck, D.; Schwarz, M.A. Shams 1-Design and operational experiences of the 100 MW–540 °C CSP plant in Abu Dhabi. *AIP Conf. Proc.* **2017**, *1850*, 020001. [[CrossRef](#)]
25. Islam, M.T.; Huda, N.; Abdullah, A.B.; Saidur, R. A comprehensive review of state-of-the-art concentrating solar power (CSP) technologies: Current status and research trends. *Renew. Sustain. Energy Rev.* **2018**, *91*, 987–1018. [[CrossRef](#)]
26. Buscemi, A.; Lo Brano, V.; Chiaruzzi, C.; Ciulla, G.; Kalogeri, C. A validated energy model of a solar dish-Stirling system considering the cleanliness of mirrors. *Appl. Energy* **2020**, *260*, 114378. [[CrossRef](#)]
27. Bădescu, V. Note concerning the maximal efficiency and the optimal operating temperature of solar converters with or without concentration. *Renew. Energy* **1991**, *1*, 131–135. [[CrossRef](#)]
28. Kongtragool, B.; Wongwiset, S. Optimum absorber temperature of a once-reflecting full conical concentrator of a low temperature differential Stirling engine. *Renew. Energy* **2005**, *30*, 1671–1687. [[CrossRef](#)]
29. Ahmadi, M.H. Investigation of Solar Collector Design Parameters Effect onto Solar Stirling Engine Efficiency. *J. Appl. Mech. Eng.* **2012**, *1*, 10–13. [[CrossRef](#)]
30. Edenhofer, O.; Madrugá, R.P.; Sokona, Y.; Seyboth, K.; Matschoss, P.; Kadner, S.; Zwickel, T.; Eickemeier, P.; Hansen, G.; Schlömer, S.; et al. *Renewable Energy Sources and Climate Change Mitigation: Special Report of the Intergovernmental Panel on Climate Change*; Cambridge University Press: Cambridge, UK, 2011; ISBN 9781139151153.

31. International Energy Agency (IEA). Data and Statistics. Available online: <https://www.iea.org/data-and-statistics/data-tables> (accessed on 1 April 2022).
32. Lemmon, E.W.; Bell, I.H.; Huber, M.L.; McLinden, M.O. *NIST Standard Reference Database 23: Reference Fluid Thermodynamic and Transport Properties-REFPROP, Version 10.0*, National Institute of Standards and Technology; Standard Reference Data Program: Gaithersburg, MD, USA, 2018.
33. Crespo, L. Chapter 13-The long-term market potential of concentrating solar power systems. In *Concentrating Solar Power Technology*, 2nd ed.; Lovegrove, K., Stein, W., Eds.; Woodhead Publishing Series in Energy; Woodhead Publishing: Sawston, UK; pp. 477–509; ISBN 978-0-12-819970-1.
34. Pfeifroth, U.; Kothe, S.; Trentmann, J.; Hollmann, R.; Fuchs, P.; Kaiser, J.; Werscheck, M. Surface Radiation Data Set-Heliosat (SARAH)-Edition 2.1. In *Satellite Application Facility on Climate Monitoring*; Global Framework for Climate Services Office: Geneva, Switzerland, 2019. [[CrossRef](#)]
35. Sengupta, M.; Xie, Y.; Lopez, A.; Habte, A.; Maclaurin, G.; Shelby, J. The National Solar Radiation Data Base (NSRDB). *Renew. Sustain. Energy Rev.* **2018**, *89*, 51–60. [[CrossRef](#)]
36. Kothe, S.; Hollmann, R.; Pfeifroth, U.; Träger-Chatterjee, C.; Trentmann, J. The CM SAF R Toolbox—A Tool for the Easy Usage of Satellite-Based Climate Data in NetCDF Format. *ISPRS Int. J. Geo-Inf.* **2019**, *8*, 109. [[CrossRef](#)]
37. Buscemi, A.; Guarino, S.; Ciulla, G.; Lo Brano, V. A methodology for optimisation of solar dish-Stirling systems size, based on the local frequency distribution of direct normal irradiance. *Appl. Energy* **2021**, *303*, 117681. [[CrossRef](#)]
38. Polo, J.; Estalayo, G. Impact of atmospheric aerosol loads on Concentrating Solar Power production in arid-desert sites. *Sol. Energy* **2015**, *115*, 621–631. [[CrossRef](#)]
39. Nikitidou, E.; Kazantzidis, A.; Salamalikis, V. The aerosol effect on direct normal irradiance in Europe under clear skies. *Renew. Energy* **2014**, *68*, 475–484. [[CrossRef](#)]
40. Viswanathan, B. Natural Gas. In *Energy Sources*; Newnes: Boston, MA, USA, 2017; pp. 59–79. [[CrossRef](#)]
41. Altawell, N. (Ed.) Chapter 4—Natural gas. In *Rural Electrification*; Academic Press: Cambridge, MA, USA, 2021; pp. 81–89; ISBN 978-0-12-822403-8.
42. Blázquez, C.S.; Borge-Diez, D.; Nieto, I.M.; Martín, A.F.; González-Aguilera, D. Multi-parametric evaluation of electrical, biogas and natural gas geothermal source heat pumps. *Renew. Energy* **2021**, *163*, 1682–1691. [[CrossRef](#)]
43. Bernardi, A.; Graciano, J.E.A.; Chachuat, B. Production of chemicals from syngas: An enviro-economic model-based investigation. *Comput. Aided Chem. Eng.* **2019**, *46*, 367–372. [[CrossRef](#)]
44. Bain, R.L.; Broer, K. *Gasification*; U.S. Department of Energy Office of Scientific and Technical Information: Oak Ridge, TN, USA, 2011; ISBN 9780470721117.
45. Solarte-Toro, J.C.; Chacón-Pérez, Y.; Cardona-Alzate, C.A. Evaluation of biogas and syngas as energy vectors for heat and power generation using lignocellulosic biomass as raw material. *Electron. J. Biotechnol.* **2018**, *33*, 52–62. [[CrossRef](#)]
46. Kitzler, H.; Pfeifer, C.; Hofbauer, H. Pressurized gasification of woody biomass—Variation of parameter. *Fuel Process. Technol.* **2011**, *92*, 908–914. [[CrossRef](#)]
47. Roddy, D.J.; Manson-Whitton, C. *Biomass Gasification and Pyrolysis*; Elsevier: Amsterdam, The Netherlands, 2012; Volume 5, ISBN 9780080878737.
48. Messineo, A.; Volpe, R.; Asdrubali, F. Evaluation of Net Energy Obtainable from Combustion of Stabilised Olive Mill By-Products. *Energies* **2012**, *5*, 1384–1397. [[CrossRef](#)]
49. Giuliano, A.; Freda, C.; Catizzone, E. Techno-economic assessment of bio-syngas production for methanol synthesis: A focus on the water–gas shift and carbon capture sections. *Bioengineering* **2020**, *7*, 70. [[CrossRef](#)] [[PubMed](#)]